Romanian Reports in Physics, Vol. 64, No. 1, P. 94–104, 2012

THE RESPONSE FUNCTION OF ISOCART (ORTEC) GAMMA-RAY SPECTROMETRY SYSTEM USING MONTE CARLO SIMULATIONS*

DANIELA GURAU[1] and OCTAVIAN SIMA[2]

[1]"Horia Hulubei" National Institute of Physics and Nuclear Engineering, P.O. Box MG-6, RO-077125, Bucharest-Magurele, Romania, E-mail: daniela.gurau@ymail.com
[2]Physics Department, Bucharest University, P.O. Box MG-11, RO-077125, Bucharest-Magurele, Romania, E-mail author 2: octavianalexandru.sima@g.unibuc.ro

Received November 20, 2010

Abstract. The routine operation and maintenance of nuclear facilities generate quantities of radioactive material in many different matrices that are packed in many different sized containers. The waste is often packaged in large containers, such as 220 l drums, because process operators find drums more economical to handle than small containers. Based on regulations, the radioactivity and the radionuclide composition of the waste should be characterized before moving, shipping offsite, burying, or placing in a storage area. The most important step of the characterization process, establishing radionuclide content, is often achieved by nondestructive assay (NDA). In this work calculation techniques useful for the calibration and evaluation of measurements of radioactive waste drums by gamma-ray spectrometry were developed. To this end, a simulation program based on GEANT 3.21 toolkit was developed to simulate the response function of ISOCART gamma-ray spectrometry system for a geometry measurement with the drum volume divided in 40 volume elements. The Monte Carlo method was applied to obtain the expected spectra in the energy range from 50 to 2000 keV, the full energy peak efficiencies and the total efficiencies for sources uniformly distributed in each of the volume elements defined within the drum as well as for the source uniformly distributed in the entire drum.

Key words: gamma-ray spectrometry, HPGe detectors, GEANT 3.21, detection efficiency, waste drums.

1. INTRODUCTION

Regulatory agencies governing the disposal of nuclear waste require that the waste be appropriately characterized prior to disposal. Based on regulations, the radioactivity and the nuclide composition of the waste should be identified before moving, shipping offsite, burying, or placing in a storage area. The most important

* Paper presented at the Annual Scientific Session of Faculty of Physics, University of Bucharest, June 18, 2010, Bucharest-Măgurele, Romania.

step of the characterization process establishing radionuclide content is often achieved by nondestructive assay (NDA). Current methods for the NDA of radioactive waste in 220 l drums rely on the assumption that both the drum matrix and the activity are homogeneously distributed within the drum. When this condition is not met and the matrix is non-homogeneous, large assay errors can result. A number of researchers have studied the calibration techniques of gamma spectrometry for the radioactive waste drums [1-13]. Several techniques based on gamma-ray measurements are commonly available and of great utility in this area, which specifically provide simple and cost-effective solutions to these gamma-ray measurement problems. For example ORTEC developed the following techniques: ISOCART, QED, SGS and TGS [14]. Among them, the ISOCART method for waste assay is the most versatile in its ability to measure a wide range of waste containers including large containers and objects that can only be measured in situ.

For health physics, engineering, industry and environmental measurements, an HPGe detector is one of the most fundamental instruments among all the radiation detection systems used. The knowledge of the detection efficiency which varies strongly with the source to detector distance, due to the geometry and absorption factors, is essential for operating these systems. The experimental efficiency calibration by the use of a specific standard source provides by far the most accurate calibration in any measurement configuration [15]. However, sometimes it can be difficult or even impossible to apply experimental calibration in the case of volume samples because the calibration source should be physically and chemically similar to the measured samples and should have similar activity distribution. Furthermore, volume calibration sources are expensive (especially if different sources are used for each configuration that should be calibrated), the calibration process is time consuming, and safety problems may arise in connection with source manipulation and storage. Therefore computational methods for efficiency calibration are most valuable especially in the case of assessment of volume sources.

Monte Carlo simulation is nowadays a powerful method for solving problems concerning radiation transport. Its application for the computation of detection efficiency has dramatically increased in the last period. The method is powerful and flexible, as it can be applied to any germanium detector, to sources of arbitrary geometry and matrix. On the other hand, a lack of precise input data can yield significant errors in the detector efficiency calibration [1, 16-18], because the values of the efficiency obtained by direct Monte Carlo computation are very sensitive to several parameters of the detector, to the cross section data, and to specific approximations implemented in the Monte Carlo model [18, 19]. In spite of the widespread application of Monte Carlo simulation for efficiency calibration of HPGe detectors for measurements of samples with the volume up to several dm^3, realistic computations by Monte Carlo methods were not previously reported for the measurement of big volume samples like 220 l waste drums.

In this paper we developed a calculation technique based on realistic Monte Carlo simulation useful for the calibration and the evaluation of measurements of radioactive waste with drum counting systems. Specifically a simulation program based on GEANT 3.21 toolkit was developed to simulate the response function of ISOCART gamma-ray spectrometry system for a geometry measurement with the drum volume divided in 40 volume elements. The Monte Carlo method was applied to obtain the expected spectra in the energy range from 50 to 2000 keV, the full energy peak efficiencies and the total efficiencies for sources uniformly distributed in each of the volume elements defined within the drum as well as for the source uniformly distributed in the entire drum.

2. THE SYSTEM DESCRIPTION

According to the Ortec online documentation [14] the ISOCART method for waste assay is the most versatile in its ability to measure a wide range of waste containers including large containers and objects that can only be measured in situ. It is also the gamma-ray assay system with the lowest instrument cost. At the same time, the ISOCART method may be the least precise with the largest errors, due to many assumptions that must be made, if the sample is highly inhomogeneous, or has low level of activity.

The ISOCART system (Fig. 1) used in this study is based on a coaxial p-type (GEM25P4) detector, reprocessed in 2007 by Ortec. The performance specifications of the detector are: relative efficiency is 25%; resolution at 1332 keV (^{60}Co) is 1.85 keV and at 122 keV (^{57}Co) is 0.82 keV. The diameter of the germanium crystal is 57.4 mm and the length 52.2 mm. The thickness of the dead layer is 0.7 mm on top and sides. A central hole is drilled into the back side of the crystal with 34 mm length and 9 mm diameter. The crystal is encased in aluminum housing with thickness equal to 1.27 mm on top and sides. The distance from end cap to crystal is 3 mm. In the measurement of waste drums this detector is shielded with a lead collimator of 203 mm length, 16 mm thickness and 110 mm inner diameter. The distance from the front of the collimator to the front of the detector is the depth dimension of 20 mm. The radioactive source considered was a 220 l cylindrical waste container with dimensions of 880 mm length and 570 mm diameter, encased in an iron container with walls having the thickness of 1.25 mm. The source matrix considered is concrete with standard composition. The axis of the detector (horizontal) is perpendicular on the axis of the cylinder (vertical); the center of the drum is located at the intersection of the two axes. The distance from the center of the coordinate system associated to the detector to the center of the cylinder is 500 mm.

3. THE GEANT 3.21 SIMULATION SETUP

The process applied in this work is based on the method similar with the tomography procedure. In view of investigating the effect of various radioactive source distributions within the drum, we considered the drum volume divided into many volume elements which are each independently submitted to simulations, so we carried out a lot of Monte Carlo simulations.

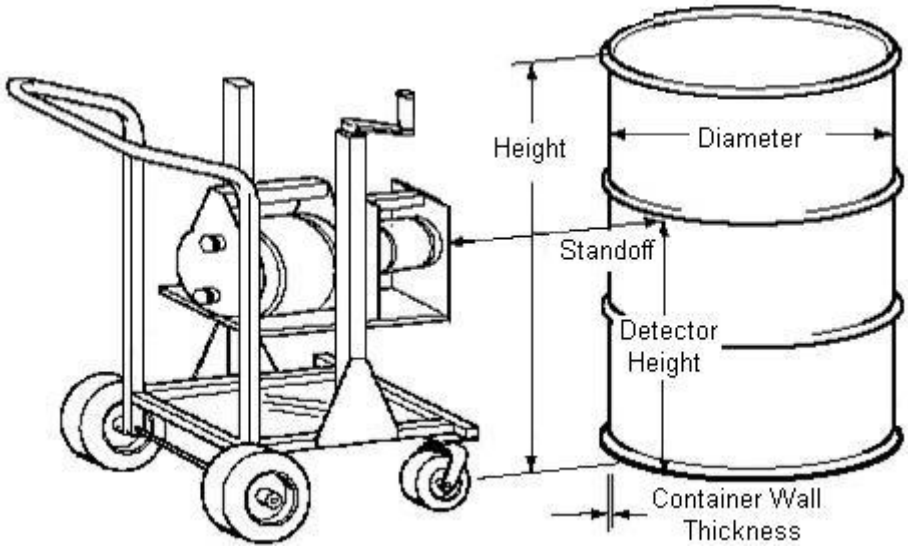

Fig. 1 – The ISOCART measurement geometry representation (from the ISOTOPIC Program for Radioactive Waste Characterization).

The volume elements were defined by applying two divisions of the volume of the drum. The first division, (a), comprising 8 cylindrical segments of 110 mm length each and radius equal to the radius R of the drum, is obtained by sectioning the drum with equidistant horizontal planes perpendicular on the drum axis. The segments are indexed from one base to the other of the drum as S1 to S8. The second division, (b), comprising an inner cylinder and four tubes, concentric with the drum axis, is obtained by defining equidistant cylindrical surfaces of radii $R_k = k \times R/5$, $k = 1$ to 5, as boundaries of the domains; each domain has the length equal to the length of the drum. In this division the domains are indexed as V1 (the inner cylinder) to V5 (the outermost tube).

The simulation of a particular system by GEANT 3.21 [21] is achieved by defining the problem of interest with the help of several user routines. In our case, first the geometry of the experimental setup was defined by specifying the detector structure (shape and dimensions, including the dead layer, the detector holder, and the end cap), the shield and the collimator, the drum (including the walls) and the

relative position of all the volumes. Then for each volume the material data were given. These input data were implemented into the geometry and material user routines of GEANT. In each run the task of the program was to evaluate the energy deposited in the sensitive volume of the detector. The complete definition of each run required also the specification of the volume element from the drum in which the radioactive source was distributed, the energy and the number of source photons to be traced. For each volume element the simulations were done for 11 photon energies: 59.54 keV (^{241}Am), 661.66 keV (^{137}Cs), 1173.24 and 1332.50 keV (^{60}Co) and 121.78, 344.28, 778.90, 964.08, 1085.84, 1112.08 and 1408.01 keV (^{152}Eu). For each energy 1.2 10^{10} photons were traced in total for the 40 volume elements, that is 1.32 10^{11} photons in total for all energies.

Basically the simulation proceeded as follows. One of the domains S1, ... S8, or V1, ...V5 was selected for the current computation. A random emission point was sampled in the selected domain, considering that the radioactivity is uniformly distributed in that domain. Of course, the volume elements S1, ... S8, V1, ...V5 were used only for the definition of the radioactive source, from the point of view of the photon interactions always the complete drum was considered. The direction of the emitted photon was randomly selected from an isotropic distribution. The transport of the source photon, as well as of each secondary photon and electron resulting from interactions in the drum, detector and the other media traversed by the radiations was followed by a realistic simulation of all the relevant interactions. In the case of photons, photoelectric, Compton scattering, coherent (Rayleigh) scattering and pair production were specifically simulated. The lower energy cut off was 10 keV. In the case of electrons ionization, delta electron production, bremsstrahlung emission, multiple scattering, energy loss straggling were described; in the case of positrons besides the same features of course annihilation was included. Electron low energy cut off was 10 keV. Any particle was traced until its energy became low enough for it to be considered locally absorbed, or it escaped from the space region of interest. In the case when the initial source photon or any of the secondary radiations that were produced did interact within the sensitive volume of the detector, the energy deposition in the detector due to all these radiations was evaluated, with the purpose of collecting the ideal energy spectrum of the detector. Then the deposited energy was distorted according to a gaussian distribution closely matching detector resolution in view of constructing the realistic energy spectrum of the detector. The procedure was repeated by selecting a new emission point and following the transport of the photon and of the associated secondary radiations by as many times as specified in the input file. In fact, due to the long computer time required, instead of making a single computation for 1.2 10^{10} source photons for each energy, several runs for a smaller number of source photons were carried out in each case and finally the partial results were combined in a single file.

In the end the ideal and the realistic spectra were obtained for each energy and for each source domain. Also, the full energy peak efficiencies and the total efficiencies were evaluated in the same cases. It is important to mention that the realistic spectra, obtained by applying an appropriate energy resolution and a typical number of channels, are similar to the experimental data and consequently may be processed with the same software as the measured spectra. Realistic spectra obtained by simulation are also useful for the analysis of specific features of the spectra, *e.g.* for the appropriate evaluation of the contribution of small angle Compton scattering to the background under the peaks, which is especially important for volume sources and low energy photons.

4. RESULTS AND DISCUSSIONS

In this work the response function of the ISOCART gamma-ray spectrometry system was studied. The Monte Carlo based GEANT 3.21 code was used for the computation of the efficiency and for the simulation of the spectra.

From the simulations the results (spectra, efficiencies) were obtained independently for 40 different source domains (the sub-domains obtained by both divisions of the drum, the eight segments and the five concentric domains – the inner cylinder and the four tubes). In this paper only the results corresponding to the complete domains S1, ... S8 and V1, ... V5 will be presented. They were computed by combining the results corresponding to the sub-domains included in the domain of interest. For example, in the case of the inner cylinder V1 the values corresponding to the sub-domains defined by the part of the segments S1 to S8 included in the V1 volume were combined together.

In Table 1 the values of the peak efficiency for the cylinder and the four tubes are presented.

Table1

The peak efficiency values for the cylinder and the four tubes

Energy (keV)	**Peak efficiency**				
	Cylinder	**Tube1**	**Tube 2**	**Tube 3**	**Tube 4**
59.54	0.00E+00	0.00E+00	0.00E+00	2.61E-07	1.69E-05
121.78	6.45E-08	4.03E-07	2.49E-06	1.77E-05	1.28E-04
344.28	1.29E-06	3.00E-06	9.86E-06	3.13E-05	1.04E-04
661.66	3.55E-06	6.50E-06	1.38E-05	3.73E-05	9.09E-05
778.90	4.44E-06	7.75E-06	1.55E-05	3.53E-05	9.32E-05
964.08	6.94E-06	9.55E-06	1.82E-05	3.76E-05	9.76E-05
1085.84	8.31E-06	1.07E-05	1.93E-05	3.93E-05	9.88E-05
1112.08	9.36E-06	1.19E-05	1.96E-05	3.93E-05	9.83E-05
1173.24	7.84E-06	1.15E-05	2.07E-05	4.00E-05	9.96E-05
1332.50	1.05E-05	1.35E-05	2.32E-05	4.26E-05	1.01E-04
1408.01	1.08E-05	1.42E-05	2.39E-05	4.36E-05	1.02E-04

In Fig. 2 the peak and total efficiency curves for the cylinder and the four tubes are presented.

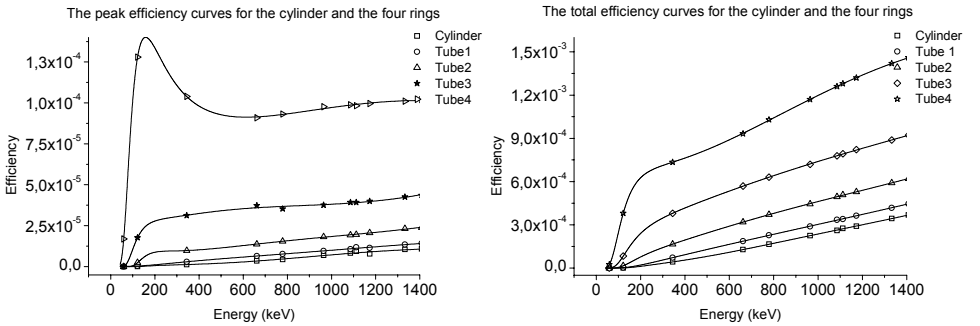

Fig. 2 – The peak (left) and total (right) efficiency curves for the cylinder and the four tubes.

As it can be seen in Fig. 2 the efficiencies are smaller for the inner cylinder and greater for the outer tube. The systematic increase of the efficiency when the source is distributed in volume elements closer and closer to the surface of the drum (from the inner cylinder to the outer tube) is easily explained by the increase of the mean solid angle and the decrease in the attenuation in the drum. Concerning the energy dependence of the efficiency curve for a given source distribution, this is the result of the energy dependence of the attenuation in the drum and of the energy dependence of the intrinsic efficiency curve of the detector. The attenuation in the drum is constantly decreasing with increasing energy of the photons, consequently more and more photons can escape from the drum as the energy increases, potentially contributing to the detector signal. The relative effect is more pronounced in the case of sources distributed far from the surface of the drum than in the case of sources distributed closer to the surface of the drum (*e.g.* the outermost tube V5); indeed, in the latter case an important fraction of the detected photons come from emission points located close to the surface and for these photons the path length through the drum is short and the attenuation is less important. The intrinsic efficiency curve for a p-type detector increase first with the energy, reaching a maximum at 100 – 200 keV [15], then decreases slowly. The initial increase is the result of a smaller attenuation in the Ge dead layer, in the end cap etc. as the energy increases, while at these energies the photons that succeed to penetrate to the sensitive volume of the detector are fully absorbed with a high probability. At higher energies the attenuation in the Ge dead layer and in the end cap is negligible, but the probability of full absorption of the photons in the sensitive volume of the detector decreases with increasing energy. The final energy dependence of the efficiency for the sources considered in this work results from the balance of the two factors. In the case of the inner cylinder and of the inner tubes the attenuation in the drum is always the dominating factor and the efficiency

increases constantly with photon energy, which is atypical for efficiency curves. In the case of the outermost tube the contribution of the emission points located close to the surface of the drum is less affected by attenuation in the drum; therefore the energy dependence of the intrinsic efficiency shows up in the final full energy peak efficiency curve, by the initial increase and then the decrease of the efficiency up to about 600 keV.

In Table 2 the values of peak efficiency for the eight segments are presented.

Table 2

The peak efficiency values for the eight segments

Energy (keV)	**Peak efficiency**							
	Segment							
	1	**2**	**3**	**4**	**5**	**6**	**7**	**8**
59.54	0.00E+00	0.00E+00	1.79E-09	8.55E-06	8.56E-06	2.30E-09	0.00E+00	0.00E+00
121.78	0.00E+00	0.00E+00	3.18E-07	7.46E-05	7.37E-05	3.12E-07	0.00E+00	0.00E+00
344.28	6.51E-08	5.56E-08	1.21E-06	7.34E-05	7.34E-05	1.15E-06	5.20E-08	7.27E-08
661.66	2.45E-06	3.38E-06	9.17E-06	6.25E-05	6.31E-05	5.41E-06	3.51E-06	2.48E-06
778.90	3.62E-06	5.21E-06	7.98E-06	6.17E-05	6.13E-05	7.89E-06	4.96E-06	3.51E-06
964.08	4.85E-06	7.12E-06	1.13E-05	6.11E-05	6.16E-05	1.15E-05	7.48E-06	4.94E-06
1085.84	5.47E-06	8.30E-06	1.29E-05	6.19E-05	6.10E-05	1.31E-05	8.15E-06	5.52E-06
1112.08	5.82E-06	8.48E-06	1.39E-05	6.16E-05	6.03E-05	1.41E-05	8.59E-06	5.76E-06
1173.24	6.01E-06	8.78E-06	1.40E-05	6.10E-05	6.08E-05	1.38E-05	8.94E-06	6.24E-06
1332.50	6.97E-06	1.06E-05	1.65E-05	6.18E-05	6.20E-05	1.64E-05	1.01E-05	6.80E-06
1408.01	7.33E-06	1.07E-05	1.68E-05	6.16E-05	6.21E-05	1.74E-05	1.09E-05	7.24E-06

In Fig. 3 the peak and total efficiency curves for the eight segments are presented.

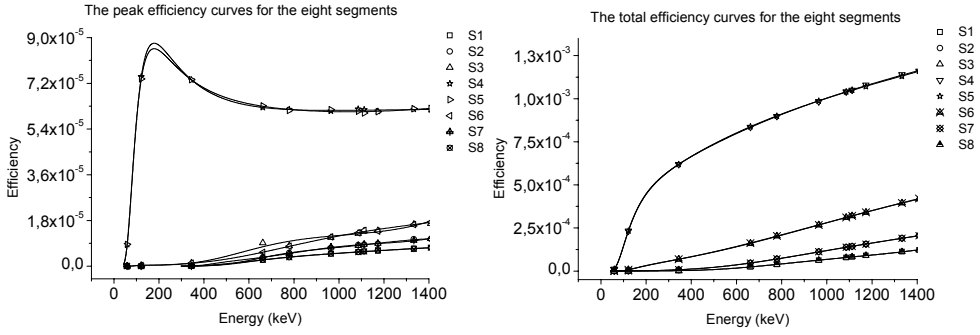

Fig. 3 – The peak (left) and total (right) efficiency curves for the eight segments.

In Fig. 4 the corresponding peak efficiency curves and the total efficiency curves simulated for the entire drum are presented.

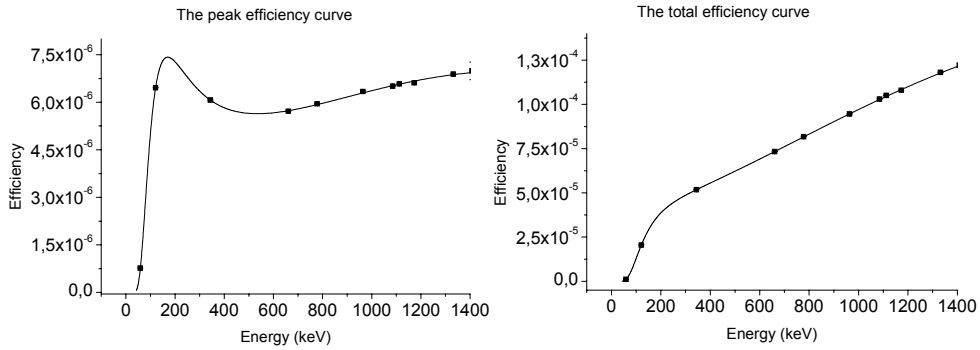

Fig. 4 – The peak (left) and total (right) efficiency curves for the drum .

Qualitatively the results displayed in Fig. 2 and Fig. 3 can be explained with similar arguments as the results displayed in Fig. 1. The segments S4 and S5 are located in front of the detector and the behavior of the efficiency curve is similar to the case of the V5 outermost cylinder. The segments S1 and S8 are farthest from the detector; the photons should come towards the detector on inclined trajectories, that are longer in average and consequently the attenuation in the drum is more important. In addition, the solid angle considerations explain the smaller values of the efficiency for the segments S1 and S8. The case of the entire drum is closer to the case of the source distributed in the V5 tube. The more important increase in the efficiency as the energy increases in the case of the entire drum than in the case of V5 is a consequence of an increase with energy of the effective volume of the active source, defined as the volume from where the emitted photons can contribute significantly to the peak efficiency.

The uncertainty obtained for the simulated efficiencies are in the range 0.13÷4.0% for peak efficiencies and 0.03÷1% for total efficiencies.

5. CONCLUSIONS

In this study the spectra and the peak and total efficiencies for several distributions of the radioactive source in a waste drum container were obtained by realistic Monte Carlo simulation. The code used was GEANT 3.21. The simulations were done for 11 photon energies and for sources distributed in 8 cylindrical segments and 5 concentric domains defined within the drum. The magnitude of the full energy peak efficiency and the energy dependence of the efficiency curves were displayed and discussed. The procedure will be used in future studies for the interpretation of the results obtained concerning the dispersion of the activity in the drum.

REFERENCES

1. P. Filβ, *Relation between the activity of a high-density waste drum and its gamma count rate measured with an unshielded Ge-detector*, Applied Radiation and Isotopes, **46**, *8*, pp. 805–812 (1995).
2. J.H. Liang, S.H. Jiang, G.T. Chou, *A theoretical investigation of calibration methods for radwaste radioactivity detection systems*, Applied Radiation and Isotopes, **47**, *7*, pp. 669–675 (1996).
3. J.H. Liang, S.H. Jiang, J.T. Chou, C.C. Chen, S.W. Lin, C.H. Lee, S.T. Chiou, *Parametric study of shell-source method for calibrating radwaste radioactivity detection systems*, Applied Radiation and Isotopes, **49**, *4*, pp. 361–368 (1998).
4. M. Bruggeman, J. Gerits, R. Carchon, *A minimum biased shell-source method for the calibration of rad-waste assay systems*, Applied Radiation and Isotopes, **51**, *3*, pp. 255–259 (1999).
5. M. Bruggeman, R. Carchon, *Solidang, a computer code for the computation of the effective solid angle and correction factors for gamma spectroscopy-based waste assay*, Applied Radiation and Isotopes, **52**, *3*, pp. 771–776 (2000).
6. L. Dinescu, I. Vata, I.L. Cazan, R. Macrin, Gh. Caragheorgheopol, Gh. Rotarescu, *On the efficiency calibration of a drum waste assay system*, Nuclear Instruments and Methods in Physics Research, **A 487**, pp. 661–666 (2002).
7. O. Sima, I.L. Cazan, L. Dinescu, D.Arnold, *Efficiency calibration of high volume samples using the GESPECOR software*, Applied Radiation and Isotopes, **61**, pp. 123–127 (2004).
8. M. Toma, O. Sima, C. Olteanu, *Experimental and simulated studies for the calibration of a radioactive waste assay system*, Nuclear Instruments and Methods in Physics Research, A **580**, *1*, pp. 391–395 (2007).
9. Y.F. Bai, E. Mauerhofer, D.Z. Wang, R. Odoj, *An improved method for the non-destructive characterization of radioactive waste by gamma scanning*, Applied Radiation and Isotopes, **67**, *10*, 1897–1903 (2009).
10. T.Q. Dung, N.D.Thanh, L.A. Tuyen, L.T. Son, P.T. Phuc, *Evaluation of a gamma technique for the assay of radioactive waste drums using two measurements from opposing directions*, Applied Radiation and Isotopes, **67**, *1*, 164–169 (2009).
11. M.C. Yuan, C.H. Yeh, J.J. Wang, I.J. Chen, C.F. Wang, *The calibration and evaluation of a radioactive waste drum counting system*, Applied Radiation and Isotopes, **67**, *5*, 931–934 (2009).
12. D. Stanga, D. Radu, O. Sima, *A new model calculation of the peak efficiency for HPGe detectors used in assays of radioactive waste drums*, Applied Radiation and Isotopes, **68**. *7–8*, 1418–1422 (2010).
13. M. Toma, C. Cristache, L. Done, F. Dragolici, O. Sima, *Characterization studies of radioactive waste drums using high resolution gamma spectrometric systems*, AIP Conference Proceedings, **1203**, pp. 35–39 (2010).
14. *** http://ortec-online.com
15. K. Debertin, R.G. Helmer, *Gamma- and X-Ray Spectrometry with Semiconductor Detectors*, North-Holland, Amsterdam, 1988, pp. 205–258.
16. R.G. Helmer, J.C. Hardy, V.E. Iacob, M. Sanchez-Vega, R.G. Neilson, J. Nelson, *The use of Monte Carlo calculations in the determination of a Ge detector efficiency curve*, Nuclear Instruments and Methods in Physics Research, **A 511**, pp. 360–381 (2003).
17. D. Arnold, O. Sima, *Extension of the efficiency calibration of the germanium detectors using the GESPECOR software*, Applied Radiation and Isotopes, **61**, pp. 117–121 (2004).
18. R.G. Helmer, N. Nica, J.C. Hardy, V.E. Iacob, *Precise efficiency calibration of an HPGe detector up to 3.5 MeV, with measurements and Monte Carlo calculations*, Applied Radiation and Isotopes, **60**, pp. 173–177 (2004).

19. T. Vidmar, I. Aubineau-Laniece, M.J. Anagnostakis, D. Arnold, R. Brettner-Messler, D. Budjas, M. Capogni, M.S. Dias, L.E. De Geer, A. Fazio, J. Gasparro, M. Hult, S. Hurtado, M. Jurado Vargas, M. Laubenstein, K.B. Lee, Y.N. Lee, M.C. Lepy, F.J. Maringer, V. Medina Peyres, M. Mille, M. Moralles, S. Nour, R. Plenteda, M.P. Rubio Montero, O. Sima, C. Tomei, G. Vidmar, *An intercomparison of Monte Carlo codes used in gamma-ray spectrometry*, Applied Radiation and Isotopes, **66**, 764–768 (2008).
20. O. Sima, D. Arnold, *On the Monte Carlo simulation of HPGe gamma-spectrometry systems*, Applied Radiation and Isotopes, **67**, 701–705 (2009).
21. R. Brun, F. Bruyant, M. Maire, A.C. McPherson, P. Zanarini, *GEANT3, Geneva: CERN Data Handling Division*, DDD/EE/84-1 (1987).